Evolution of the scintillation index and the optical vortex density in speckle fields after removal of the least-squares phase

Mingzhou Chen[1,*] and Filippus S. Roux[2,3]

[1]*Applied Optics, School of Physics, National University of Ireland Galway, University Road, Galway, Ireland*
[2]*National Laser Centre, CSIR, P.O. Box 395, Pretoria 0001, South Africa*
[3]*E-mail: fsroux@csir.co.za*
[*]*Corresponding author: mingzhou.chen@nuigalway.ie*

Received June 29, 2010; accepted August 5, 2010;
posted August 12, 2010 (Doc. ID 130893); published September 8, 2010

Knowledge of the behavior of stochastic optical fields can aid the understanding of the scintillation of light propagating through a turbulent medium. For this purpose, we perform a numerical investigation of the evolution of the scintillation index and the optical vortex density in a speckle field after removing its continuous phase. We find that both the scintillation index and the vortex density initially drop and then increase again to reach an equilibrium level. It is also found that the initial rate of decrease in both cases is 1 order of magnitude faster than the eventual rate of increase. Their detail shapes are however different. Therefore different empirical functions are used to fit the shapes of these curves. © 2010 Optical Society of America

OCIS codes: 030.6140, 350.5500, 350.5030, 260.6042, 030.6600.

1. INTRODUCTION

Although optical vortices [1] have found various applications, including optical measurement [2–4], trapping and manipulation of particles [5,6], free-space optical communication [7–9], quantum entanglement [10,11], and optical vortex coronagraph [12], their presence in an optical beam is not always desirable. Optical vortices appear spontaneously when coherent light is distorted severely enough by a random medium, such as a turbulent atmosphere, through which it propagates. Such vortices are located at the dark regions where the intensity vanishes and the phase is singular. Optical vortices can have either positive or negative topological charge, depending on the handedness of the phase increment around the vortex core. A pair of positive and negative vortices can be annihilated or created during free-space propagation.

To address the challenge of removing these optical vortices [13] it is necessary to understand the collective behavior of optical vortices in strongly scintillated beams, as well as in other optical vortex fields. As a starting point one can consider optical speckle fields, which are better understood.

Obtained by scattering coherent light through a highly distorted medium or by reflecting coherent light from a surface with its roughness on the scale of a wavelength, a speckle field contains a random distribution of optical vortices. The optical vortex density, which is defined as the total number of vortices per unit area and given by half the inverse of the coherence area of the speckle beam [14], is statistically stable along the propagation direction. The net topological charge in any finite area tends to be much smaller than the total number of vortices in that area, especially for larger areas. The topological charges of neighboring optical vortices are anti-correlated [15]. In spite of their point-like appearances, optical vortices have an influence over the whole wave field and therefore affect the global phase structure. Considering the speckle in a three-dimensional volume, one finds that the point-like vortices become lines [16–19] that can be curved, knotted, and looped, giving rise to the motion, creation, and annihilation of vortices in a two-dimensional plane perpendicular to the propagation direction. However, the rate of vortex dipole annihilation is statistically equal to the rate of vortex dipole creation so that the average vortex density remains constant during propagation. In this sense, a static speckle field represents a state of equilibrium during its free-space propagation.

It is easier to use numerical methods to study optical vortices in speckle fields [19,20] than to use experimental techniques. Far-field Gaussian speckle fields can be generated as the Fourier transform of a set of point sources having random phases [14]. Examples of different ways to simulate the illuminated sources include uniformly illuminated square envelopes, uniformly illuminated circular envelopes, and symmetric Gaussian envelopes [21,22]. Although the properties of static speckle fields have been widely investigated [14,22–29], studies of the properties of speckle fields after their equilibrium states have been destroyed are rare.

Our approach to address the challenge of removing optical vortices is to first understand the underlying dynamics of optical vortices that is inherent to stochastic optical fields. Hence, in this paper, we extend our previous work [30] on optical vortices in strongly scintillated beams by considering the evolution of a speckle field after destroying its equilibrium state through the removal of the continuous part of its phase function. Although a speckle field differs from a scintillated optical field, an under-

standing of the dynamics of vortices in phase corrected speckle fields will enhance our understanding of similar dynamics that exist in scintillated beams. We propagate the phase corrected speckle field step by step in free-space, in a way similar to the numerical method used by Martin and Flatté in their study of laser beams propagating in random media [31,32]. Both the scintillation index and the vortex density are used in our study of the evolution of phase corrected speckle fields.

2. MATHEMATICAL BACKGROUND

A speckle is obtained from a coherent superposition of multiple plane waves with a random angular spectrum, restricted to a region around the origin of the spatial frequency domain. The size of this region is inversely proportional to the coherence area of the speckle beam. A speckle field $\psi(\mathbf{x})$ can therefore be written as

$$\psi(\mathbf{x}) = \int\int_{-\infty}^{\infty} \alpha(\mathbf{a})\exp(-i2\pi\mathbf{a}\cdot\mathbf{x})\mathrm{d}^2a, \tag{1}$$

where $\mathbf{x}$ is the two-dimensional position vector on a plane perpendicular to the direction of propagation (the propagation axis is assumed to be the z-axis), $\mathbf{a}$ is the two-dimensional spatial frequency vector, and $\alpha(\mathbf{a})$ represents the random angular spectrum for the speckle beam.

In this paper a Gaussian spectral envelope is used to restrict the angular spectrum to the area around the origin, as given by

$$\alpha(\mathbf{a}) = \tilde{\chi}(\mathbf{a})\exp\left(\frac{-|\mathbf{a}|^2}{W^2}\right), \tag{2}$$

where $\tilde{\chi}(\mathbf{a})$ is a normally distributed complex-valued random function and W is a scale for the radius of the angular spectrum. The spatial coherence length L_c, which is defined here as the square root of the spatial coherence area, is inversely proportional to W.

One can express the speckle beam in terms of amplitude and phase. The phase can be separated into a continuous phase and a sum of phase singularities (optical vortices). The complex-valued speckle field is therefore expressed as

$$\psi(\mathbf{x}) = |\psi(\mathbf{x})|\exp\left[i\theta_c(\mathbf{x}) + i\sum_n \nu_n\phi(\mathbf{x}-\mathbf{x}_n)\right], \tag{3}$$

where $\theta_c(\mathbf{x})$ is the continuous phase, $\phi(\mathbf{x}-\mathbf{x}_n)$ represents a phase singularity located at $\mathbf{x}_n$, and ν_n represents the topological charge (± 1) of the phase singularity.

Here we investigate the behavior of a speckle beam after the continuous part of the phase has been removed. The separation between the continuous and singular parts of the phase is not unique. One way to do the separation is to compute the least-squares phase, which gives an optimal estimate of the continuous part of the total phase. We illustrate the process in Fig. 1. The amplitude (or the square root of the intensity) of a typical speckle field is shown in Fig. 1(a), and Fig. 1(b) presents the total phase of the speckle field $\theta(\mathbf{x})$. The least-squares phase $\theta_{\mathrm{LS}}(\mathbf{x})$, which is shown in Fig. 1(c), can be computed from

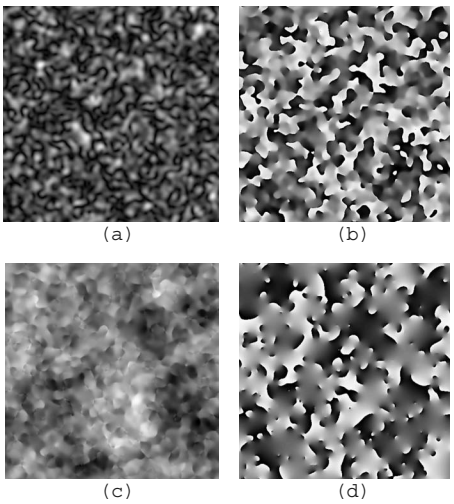

Fig. 1. Anatomy of a speckle field: (a) amplitude of the speckle field (square root of the intensity), (b) total phase of the speckle field, (c) least-squares continuous phase, and (d) the singular part of the phase of a speckle field.

the Fourier transform of the Laplacian of $\theta(\mathbf{x})$. From the Fourier theorem we know that

$$\mathcal{F}\{\nabla_T^2\theta(\mathbf{x})\} = -|\mathbf{a}|^2\mathcal{F}\{\theta(\mathbf{x})\}. \tag{4}$$

Since the phase singularities do not survive the transverse Laplacian operation ∇_T^2 [33,34], one can recover the continuous part as the least-squares phase,

$$\theta_{\mathrm{LS}}(\mathbf{x}) = -\mathcal{F}^{-1}\left\{\frac{\mathcal{F}\{\nabla_T^2\theta(\mathbf{x})\}}{|\mathbf{a}|^2}\right\}. \tag{5}$$

For the discrete case, as used in numerical simulations, this becomes

$$\theta_{\mathrm{LS}}(\mathbf{x}) = -\mathcal{F}^{-1}\left\{\frac{\mathcal{F}\{\Delta_T^2\theta(\mathbf{x})\}}{2[2-\cos(2\pi\delta_x)-\cos(2\pi\delta_y)]}\right\}, \tag{6}$$

where Δ_T^2 represents the discrete version of the transverse Laplacian and δ_x (δ_y) is the sample spacing in the Fourier domain along x (y).

The least-squares phase $\theta_{\mathrm{LS}}(\mathbf{x})$ is removed by multiplying the speckle beam with the complex conjugate of the least-squares phase. As a result the speckle field now only contains the singular part of the phase, shown in Fig. 1(d), which only consists of phase singularities. The resulting so-called phase corrected speckle field is then allowed to propagate through free-space, as explained in the next section. Note that the amplitude [Fig. 1(a)] is not directly affected by this least-squares phase removal process.

The variation in the intensity of an optical field can be quantified by the scintillation index, which is defined as the variance in the intensity divided by the square of the average intensity. In terms of the moments it is given by

$$\sigma_I = \frac{\langle I^2\rangle}{\langle I\rangle^2} - 1. \tag{7}$$

The scintillation index of a speckle field is approximately equal to 1. We will use the scintillation index, together with the vortex density, to study the evolution of the op-

tical field after the least-squares phase has been removed.

One can argue that the evolution of the vortex density or the scintillation index should become conformal in the paraxial limit, because in this limit one can formulate the propagation of light completely independent of any scale parameters. This is indeed what is observed: plotting the scintillation index or the normalized vortex density as a function of the (dimensionless) normalized propagation distance $t=z\lambda/L_c^2$, where L_c is the coherence length, one finds that the curves always have the same shape, regardless of the values of L_c or λ. Hence, in the paraxial limit the evolution of the vortex density and the scintillation index are unique and scale invariant. In this paper, we only consider the paraxial limit.

3. NUMERICAL SIMULATION

The propagation of the speckle beam after the removal of its least-squares phase was simulated with a numerical implementation of scalar diffraction theory, based on Fourier optics [35,36]. The input speckle fields are sampled complex-valued functions, consisting of 512×512 samples that represent the speckle beam in a plane perpendicular to the propagation direction. The speckle fields are produced by numerical implementations of Eqs. (1) and (2), where the starting point is a randomly generated two-dimensional array of normally distributed complex values to produce $\tilde{\chi}(\mathbf{a})$. The Fourier transform of the resulting angular spectrum $\alpha(\mathbf{a})$ then gives a speckle field with periodic boundary conditions. In other words, the opposite edges of the speckle field match each other continuously so that the field could be used to tile the infinite two-dimensional plane to produce a continuous function. As a result the speckle field does not expand during propagation. This is necessary to avoid edge effects and aliasing. Care is taken to ensure that the periodic boundary conditions are also maintained during the least-squares phase removal process and the entire propagation process.

The numerical procedure propagates the initial phase corrected speckle field through free-space over progressively larger distances. The propagation distance is increased in logarithmically increasing steps. The reason for the logarithmic dependence follows from the shapes of the resulting vortex density and the scintillation index curves. Due to a large difference in the initial rate at which these quantities decrease compared the subsequent rate at which they increase again, it is better to simulate the process at logarithmically increasing propagation distances. (The very slow rate of increase after the dip previously caused the authors to have the incorrect impression that the dip represented an equilibrium vortex density [30].) For each step the scintillation index is computed and the total number of vortices that are located inside the 512×512 sample window is determined as a function of the logarithmic propagation distance. The simulation was repeated several times for different initial speckle fields, having different coherence areas. We kept the wavelength the same (equal to one sample spacing) for all the simulations. The coherence length, which is always computed from the final vortex density V_∞ according to $L_c=(2V_\infty)^{-1/2}$, was always chosen to be large enough to ensure that all the simulations obey the paraxial approximation.

4. NUMERICAL RESULTS

The normalized optical vortex density for a phase corrected speckle field is shown in Fig. 2 as a function of linear normalized propagation distance [Fig. 2(a)], as well as logarithmic normalized propagation distance [Fig. 2(b)]. The latter makes it easier to see the final equilibrium optical vortex density. The normalized propagation distance is defined as $t=z\lambda/L_c^2$. The optical vortex density curves have been normalized before the averages and standard deviations were computed. The curve shown in Fig. 2 represents a case where $L_c=19.7\lambda$, which is well within the paraxial limit. It reveals several interesting features of the process. After the least-squares phase has been removed, the vortex density drops drastically as a function of the propagation distance. The vortex density then reaches a minimum value of about 70% of the initial vortex density. The vortex density then starts to rise again, but at a rate that is 1 order of magnitude slower than the rate at which it dropped. Finally it reaches an equilibrium value of about 88% of the initial vortex density. Perhaps the most striking feature of this curve is the large

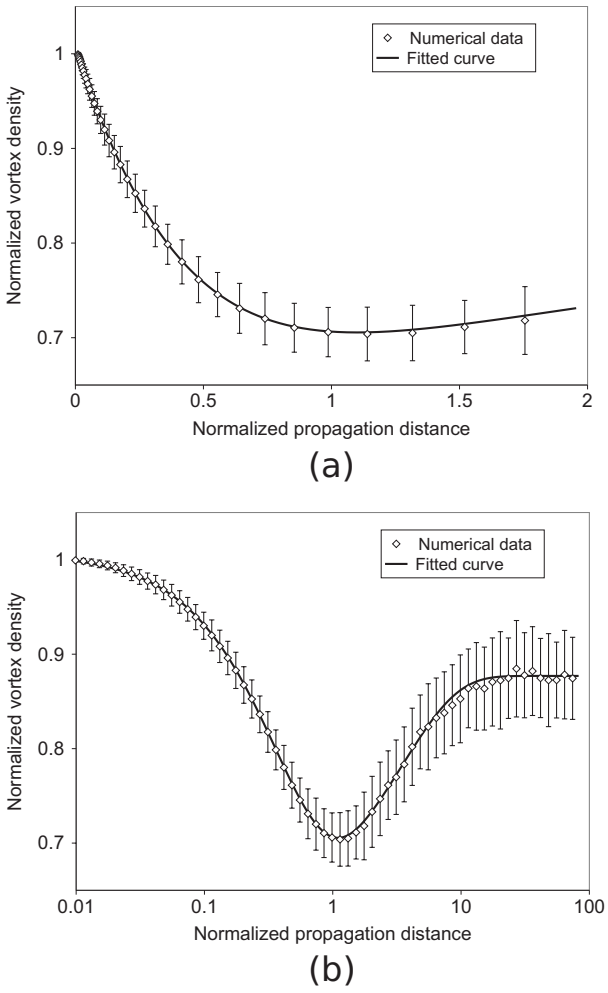

Fig. 2. Normalized optical vortex density for a phase corrected speckle field, shown as a function of (a) linear normalized propagation distance, as well as (b) logarithmic normalized propagation distance. The diamonds represent numerical data, averaged over more than a hundred different simulations. The error bars represent standard deviations. A solid curve is fitted through these data points as discussed in the text.

difference in scale between the propagation distances required to go from the initial density to the dip and from the dip to the final equilibrium value.

The numerical data obtained for the evolution of the vortex density in the paraxial limit can be fitted by the function

$$V(z) = A_0 + A_1 \exp(-K_0 z^2 - k_1 z) - A_2 \exp(-k_2 z), \quad (8)$$

where z is the propagation distance, $A_0 = 0.5/L_c^2$ (by definition), $A_1 = (0.219 \pm 0.004)/L_c^2$, $A_2 = (0.146 \pm 0.004)/L_c^2$, $K_0 = (0.50 \pm 0.09)\lambda^2/L_c^4$, $k_1 = (2.39 \pm 0.04)\lambda/L_c^2$, and $k_2 = (0.285 \pm 0.013)\lambda/L_c^2$, with λ being the wavelength and L_c being the coherence length, computed from the final equilibrium vortex density of the phase corrected speckle field. The equilibrium value of the vortex density is represented by A_0 and is by definition equal to $1/2L_c^2$ [14]. The values of the optical vortex density, which are shown in Fig. 2, are normalized with respect to the initial vortex density, which is given by $A_0 + A_1 - A_2$. Being densities, the three constants A_0, A_1, and A_2 scale as $1/L_c^2$. The way in which the remaining parameters depend on λ and L_c follows from the scaling properties in the paraxial limit. As a result the position of the minimum vortex density also scales according to the scaling properties in the paraxial limit and is given by $z_m = 1.1L_c^2/\lambda$. We do not currently have a very compelling reason why the function for the evolution of the vortex density should have the form given in Eq. (8), other than saying that one expects it to be composed of exponential functions to represent the decay process associated with the diffusion of vortices.

Figure 3 shows the evolution of the scintillation index for the same phase corrected speckle field that is considered in Fig. 2. Again curves are shown as a function of linear normalized propagation distance [Fig. 3(a)] and logarithmic normalized propagation distance [Fig. 3(b)]. The shape of the curves shows a behavior that resembles the evolution of the vortex density. After the least-squares phase has been removed, the scintillation index also drops, but it starts off more gradually than the vortex density. The scintillation index then reaches a minimum value of about 0.7, which is 70% of the initial value, similar to what is observed for the vortex density. The minimum is also located at a propagation distance that is very close to the location of the minimum vortex density. The subsequent rise in the value of the scintillation index also occurs at a rate that is much slower than the rate at which it dropped. However, the final equilibrium value is approximately equal to 1, which is the same as that it started with, meaning that the optical field has the appearance of a speckle field again.

The numerical data for the evolution of the scintillation index in the paraxial limit, which is shown in Fig. 3, can be fitted by the function

$$\sigma(z) = B_0 - B_1 \exp\left[-G \ln\left(\frac{z}{z_d} \right)^2 \right], \quad (9)$$

where $B_0 = 0.998 \pm 0.003$, $B_1 = 0.310 \pm 0.003$, $G = 0.549 \pm 0.006$, and $z_d = (1.367 \pm 0.012)L_c^2/\lambda$. The latter is the location of the minimum scintillation index along the propagation direction. The only scale parameter z_d depends on λ and L_c according to the scaling properties of the propagation distance in the paraxial limit. The other parameters B_0, B_1, and G are scale independent dimensionless constants.

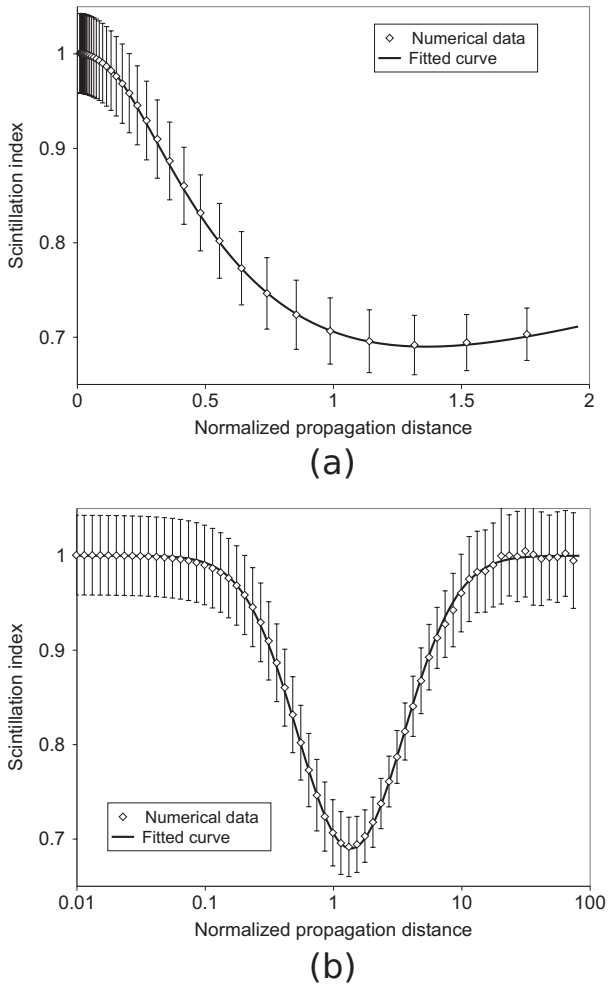

Fig. 3. Scintillation index for a phase corrected speckle field, shown as a function of (a) linear normalized propagation distance, as well as (b) logarithmic normalized propagation distance. The diamonds represent numerical data, averaged over more than a hundred different simulations. The error bars represent standard deviations. A solid curve is fitted through these data points as discussed in the text.

5. DISCUSSION

There are obvious similarities between the curves for the scintillation index (Fig. 3) and the vortex density (Fig. 2). Both show an initial drop, reaching their minima of about 70% of the initial values at roughly the same propagation distance, and then rising again at a much slower rate toward their respective equilibrium values. However, the resemblance ends here. A closer inspection of the curves shows that they are qualitatively rather different. While the vortex density starts with a fairly steep negative slope, the scintillation index appears to have a zero initial slope. Naturally the initial values of the two quantities are different. The initial vortex density depends on the speckle field before the phase removal, whereas the scintillation index is always close to 1. The equilibrium values

are also different. The scintillation index goes back to 1. The vortex density, on the other hand, settles at a lower value than its initial value.

The phase of the speckle field is changed all of the sudden when its least-squares phase is removed, while the amplitude (intensity) remains untouched. Because optical vortices are connected with the global phase structure of an optical field, the vortex density starts to change immediately after the phase removal. However, the scintillation index will not change immediately after the phase removal because it depends on the intensity. During subsequent propagation the phase changes due to the least-squares phase removal become coupled with the amplitude, which is reminiscent of an optical beam propagating in free-space after passing through a phase screen. As a result, there is always a lag in the behavior of the scintillation index with respect to the behavior vortex density (for example, z_m is slightly smaller than z_d).

The qualitative differences of these curves imply that different functions are required to fit them. While the vortex density is fitted with a bi-exponential function, shown in Eq. (8), the scintillation index is very well fitted by a Gaussian as a function of the logarithmic propagation distance, shown in Eq. (9). This reveals deeper differences between the two curves. Firstly, the scintillation index requires only one scale parameter, which is given here in terms of the location of the dip, and which is proportional to L_c^2/λ. The vortex density, on the other hand, requires at least two different scale parameters. Both are proportional to L_c^2/λ, but their proportionality constants differ by a factor of almost 1 order of magnitude. This apparent separation in scales is a fascinating observation that merits further investigation. Secondly, the initial value and slope of the scintillation index do not give information about the appearance and location of the dip. In contrast one can use the initial value and slope of the vortex density curve to solve for two of the free parameters required to fit the curve.

The shape of the vortex density curve, shown in Fig. 2, is somewhat surprising. One might have expected that the restoration of the normal speckle behavior would follow a simple exponential decay process for the vortex density after the phase correction perturbed the equilibrium. In such a case the process could be described by a first order differential equation. Instead the process follows a curve that cannot be produced by a single first order differential equation, because the slope of the function in Fig. 2 is not directly related to that function value. The curve therefore requires a second order differential equation. The second order differential equation that gives Eq. (8) as a solution is given by

$$\frac{\partial^2 V(z)}{\partial z^2} + [\kappa(z) + k_2]\frac{\partial V(z)}{\partial z} + k_2\kappa(z)[V(z) - A_0] = 0, \quad (10)$$

where

$$\kappa(z) = 2K_0 z + k_1 - \frac{2K_0}{2K_0 z + k_1 - k_2}. \quad (11)$$

The parameters A_1 and A_2 in Eq. (8) are determined by initial conditions. The rest of the parameters appear explicitly in the differential equation.

The shape of the curve for the scintillation index is less surprising, because one does expect the scintillation index to return to 1, representing a speckle at the equilibrium state. One can compare the curve for the scintillation index that is shown in Fig. 3 with the well known behavior of the scintillation index of an optical beam propagating through a turbulent medium. It is known that under such conditions the scintillation index reaches a maximum and then decreases to an equilibrium value of 1 [37]. The rate at which the peak is reached is much faster than the rate at which it then decreases until it reaches the equilibrium value. In that case the scales that govern these rates are given in terms of the scales provided by the properties of the turbulent medium. It is therefore quite surprising that a similar difference in scales is observed in the present scenario where no turbulent medium is present.

An attempt to describe the evolution of the scintillation index by a differential equation does not make sense, because one cannot solve all the free parameters required in that function from knowledge of the initial conditions. It is amusing that the shape of the evolution of the scintillation index is a mirror symmetric Gaussian function around the minimum value when plotted as a function of the logarithmic propagation distance.

6. SUMMARY

The evolution of the scintillation index and the vortex density is investigated after the least-squares phase was removed from an optical speckle field. The phase removal process serves to destroy the equilibrium in the speckle field. The investigation reveals that the scintillation index drops to a minimum and rises again to an equilibrium value of 1 as expected for a speckle field. The vortex density also initially drops to a lower value and then rises again to an equilibrium value that is lower than the initial value. In both cases the rate of increase is much slower than the initial rate at which these quantities decreased. Different functions are used to fit these curves, and a second order differential equation is proposed for the evolution of the vortex density.

ACKNOWLEDGMENT

This research was supported by the Science Foundation of Ireland under Grant No. 07/IN.1/I906.

REFERENCES

1. J. F. Nye and M. V. Berry, "Dislocations in wave trains," Proc. R. Soc. London, Ser. A **336**, 165–190 (1974).
2. W. Wang, T. Yokozeki, R. Ishijima, and M. Takeda, "Optical vortex metrology based on the core structures of phase singularities in Laguerre–Gauss transform of a speckle pattern," Opt. Express **14**, 10195–10206 (2006).
3. J. Lin and X.-C. Yuan, "Application of orbital angular momentum in optical measurement," Proc. SPIE **74300**, 74300G (2009).
4. J. Masajada, M. Leniec, S. Drobczyński, H. Thienpont, and B. Kress, "Micro-step localization using double charge optical vortex interferometer," Opt. Express **17**, 16144–16159 (2009).

5. H. He, M. E. J. Friese, N. R. Heckenberg, and H. Rubinsztein-Dunlop, "Direct observation of transfer of angular momentum to absorptive particles from a laser beam with a phase singularity," Phys. Rev. Lett. **75**, 826–829 (1995).
6. K. T. Gahagan and J. G. A. Swartzlander, "Optical vortex trapping of particles," Opt. Lett. **21**, 827–829 (1996).
7. G. Gibson, J. Courtial, M. J. Padgett, M. Vasnetsov, V. Pas'ko, S. M. Barnett, and S. Franke-Arnold, "Free-space information transfer using light beams carrying orbital angular momentum," Opt. Eng. (Bellingham) **12**, 5448–5456 (2004).
8. C. Paterson, "Atmospheric turbulence and orbital angular momentum of single photons for optical communication," Phys. Rev. Lett. **94**, 153901-1 (2005).
9. J. A. Anguita, M. A. Neifeld, and B. V. Vasic, "Turbulence-induced channel crosstalk in an orbital angular momentum-multiplexed free-space optical link," Appl. Opt. **47**, 2414–2429 (2008).
10. A. Mair, A. Vaziri, G. Weihs, and A. Zeilinger, "Entanglement of the orbital angular momentum states of photons," Nature **412**, 313–316 (2001).
11. J. Leach, B. Jack, J. Romero, M. Ritsch-Marte, R. W. Boyd, A. K. Jha, S. M. Barnett, S. Franke-Arnold, and M. J. Padgett, "Violation of a bell inequality in two-dimensional orbital angular momentum state-spaces," Opt. Express **17**, 8287–8293 (2009).
12. G. Foo, D. M. Palacios, and J. Grover A. Swartzlander, "Optical vortex coronagraph," Opt. Lett. **30**, 3308–3310 (2005).
13. M. Chen and F. S. Roux, "Accelerating the annihilation of an optical vortex dipole in a Gaussian beam," J. Opt. Soc. Am. A **25**, 1279–1286 (2008).
14. I. Freund, N. Shvartsman, and V. Freilikher, "Optical dislocation networks in highly random media," Opt. Commun. **101**, 247–264 (1993).
15. N. Shvartsman and I. Freund, "Vortices in random wave fields: nearest neighbor anticorrelations," Phys. Rev. Lett. **72**, 1008–1011 (1994).
16. M. Dennis, "Local phase structure of wave dislocation lines: twist and twirl," J. Opt. A, Pure Appl. Opt. **6**, S202–S208 (2004).
17. J. Leach, M. R. Dennis, J. Courtial, and M. J. Padgett, "Knotted threads of darkness," Nature **432**, 165–165 (2004).
18. M. V. Berry and M. R. Dennis, "Topological events on wave dislocation lines: birth and death of loops, and reconnection," J. Phys. A: Math. Theor. **40**, 65–74 (2007).
19. K. O'Holleran, M. R. Dennis, and M. J. Padgett, "Topology of light's darkness," Phys. Rev. Lett. **102**, 143902 (2009).
20. G. Sendra, H. Rabal, M. Trivi, and R. Arizaga, "Numerical model for simulation of dynamic speckle reference patterns," Opt. Commun. **282**, 3693–3700 (2009).
21. E. Ochoa and J. W. Goodman, "Statistical properties of ray directions in a monochromatic speckle pattern," J. Opt. Soc. Am. **73**, 943–949 (1983).
22. I. Freund, "Optical vortices in Gaussian random wave fields: statistical probability densities," J. Opt. Soc. Am. A **11**, 1644–1652 (1994).
23. M. Berry, "Disruption of wavefronts: statistics of dislocations in incoherent Gaussian random waves," J. Phys. A **11**, 27–37 (1978).
24. K. A. O'Donnell, "Speckle statistics of doubly scattered light," J. Opt. Soc. Am. **72**, 1459–1463 (1982).
25. I. Freund, "Saddles, singularities, and extrema in random phase fields," Phys. Rev. E **52**, 2348–2360 (1995).
26. M. R. Dennis, "Topological singularities in wave fields," Ph.D. dissertation (University of Bristol, 2001).
27. W. Wang, S. G. Hanson, Y. Miyamoto, and M. Takeda, "Experimental investigation of local properties and statistics of optical vortices in random wave fields," Phys. Rev. Lett. **94**, 103902 (2005).
28. S. Zhang, B. Hu, P. Sebbah, and A. Z. Genack, "Speckle evolution of diffusive and localized waves," Phys. Rev. Lett. **99**, 063902 (2007).
29. G. H. Sendra, H. J. Rabal, R. Arizaga, and M. Trivi, "Vortex analysis in dynamic speckle images," J. Opt. Soc. Am. A **26**, 2634–2639 (2009).
30. M. Chen and F. S. Roux, "Influence of the least-squares phase on optical vortices in strongly scintillated beams," Phys. Rev. A **80**, 013824 (2009).
31. J. M. Martin and S. M. Flatté, "Intensity images and statistics from numerical simulation of wave propagation in 3-D random media," Appl. Opt. **27**, 2111–2126 (1988).
32. J. M. Martin and S. M. Flatté, "Simulation of point-source scintillation through three-dimensional random media," J. Opt. Soc. Am. A **7**, 838–847 (1990).
33. D. C. Ghiglia and M. D. Pritt, *Two-Dimensional Phase Unwrapping: Theory, Algorithms, and Software* (Wiley, 1998).
34. D. L. Fried, "Branch point problem in adaptive optics," J. Opt. Soc. Am. A **15**, 2759–2768 (1998).
35. A. J. Devaney and G. C. Sherman, "Plane-wave representations for scalar wave fields," SIAM Rev. **15**, 765–786 (1973).
36. J. W. Goodman, *Introduction to Fourier Optics*, 3rd ed. (Roberts, 2005).
37. L. C. Andrews, R. L. Phillips, C. Y. Hopen, and M. A. Al-Habash, "Theory of optical scintillation," J. Opt. Soc. Am. A **16**, 1417–1429 (1999).